Supporting Information

Ultrahigh Permeable C_2N-Inspired Graphene Nanomesh Membranes versus Highly Strained C_2N for Reverse Osmosis Desalination

Mostafa Fakhraee and Omid Akhavan*

Department of Physics, Sharif University of Technology, P. O. Box 11155-9161, Tehran, I.R. Iran

* Corresponding author.

Tel.: +98-21-66164566

Fax: +98-21-66022711

E-mail address: oakhavan@sharif.edu (O. Akhavan)

Table S1. LJ and point charges parameters applied in the current work.

Atom type	ε / kJ.mol^{-1}	σ / nm	q / e	Reference
Cl^-	0.0489528	0.516450	-1.0000	[1]
Na^+	0.7045856	0.225890	1.0000	[1]
O_W	0.6809460	0.316435	-1.04844	[2]
H_W	0.0000000	0.000000	0.52422	[2]
C (sp^2)	0.3594056	0.339970	0.0000	[3]
C_{COH}	0.2941352	0.355000	0.2000	[4]
H_{COH}	0.0000000	0.000000	0.4400	[4]
O_{COH}	0.6485200	0.307000	-0.6400	[4]
C_{CH}	0.1924640	0.298500	-0.1150	[5]
H_{CH}	0.1259384	0.242000	0.1150	[5]
C_{C2N}	0.3598240	0.339967	0.2400	[6]
N_{C2N}	0.7112800	0.325000	-0.4800	[6]

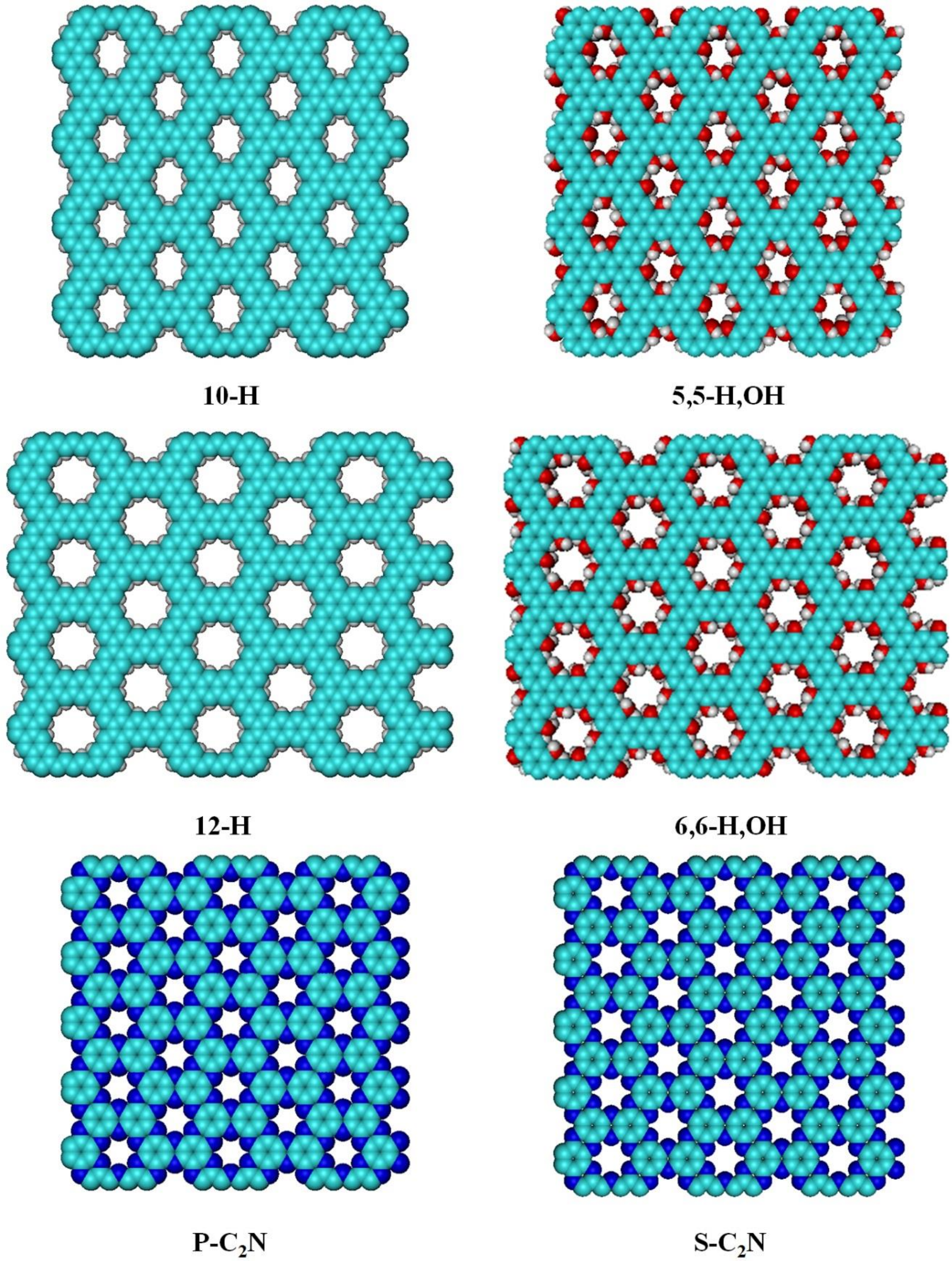

Figure S1. Selected H- and OH-passivated GNMs alongside pristine (P-C_2N) and highly strained C_2N (S-C_2N) in the current work.

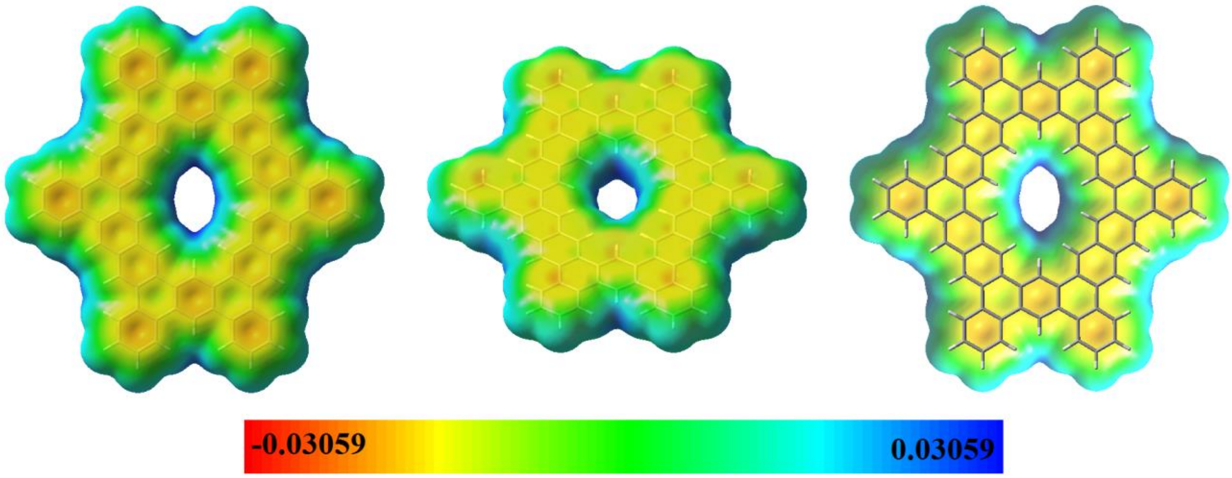

Figure S2. Electrostatic potential map (ESP) isosurfaces (isovalue of 0.0004 e/Å^3) of 10-H nanosheet achieved at the B3LYP/6-31G(d,p) theoretical level, from three point of views.

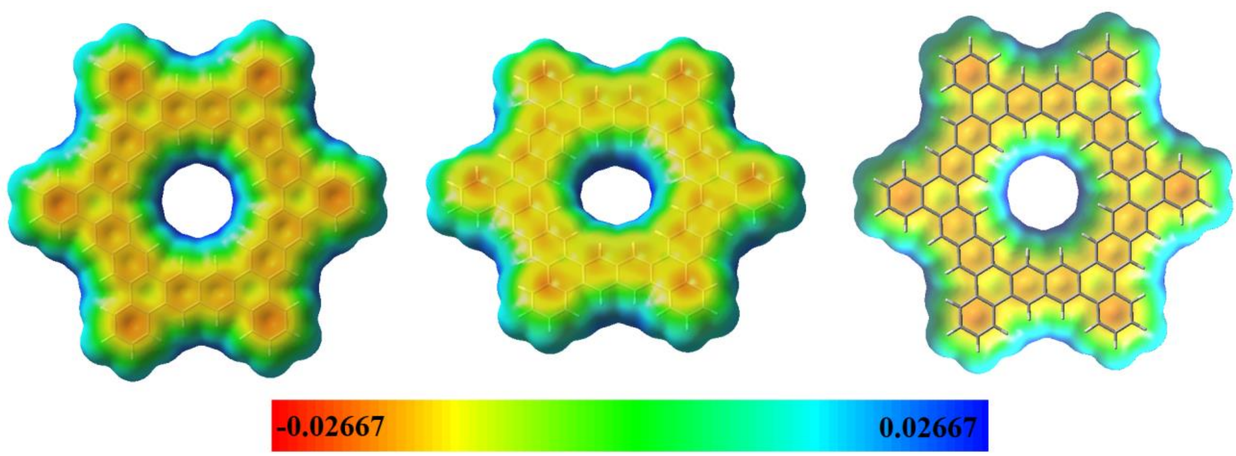

Figure S3. Electrostatic potential map (ESP) isosurfaces (isovalue of 0.0004 e/Å^3) of 12-H nanosheet achieved at the B3LYP/6-31G(d,p) theoretical level, from three point of views.

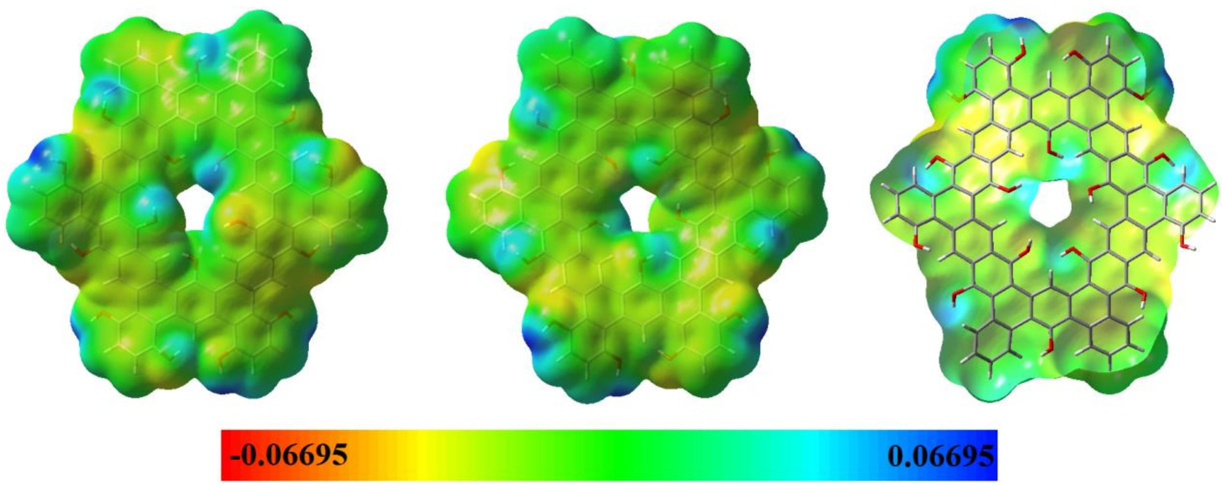

Figure S4. Electrostatic potential map (ESP) isosurfaces (isovalue of 0.0004 e/Å^3) of 5,5-H,OH nanosheet achieved at the B3LYP/6-31G(d,p) theoretical level, from three point of views.

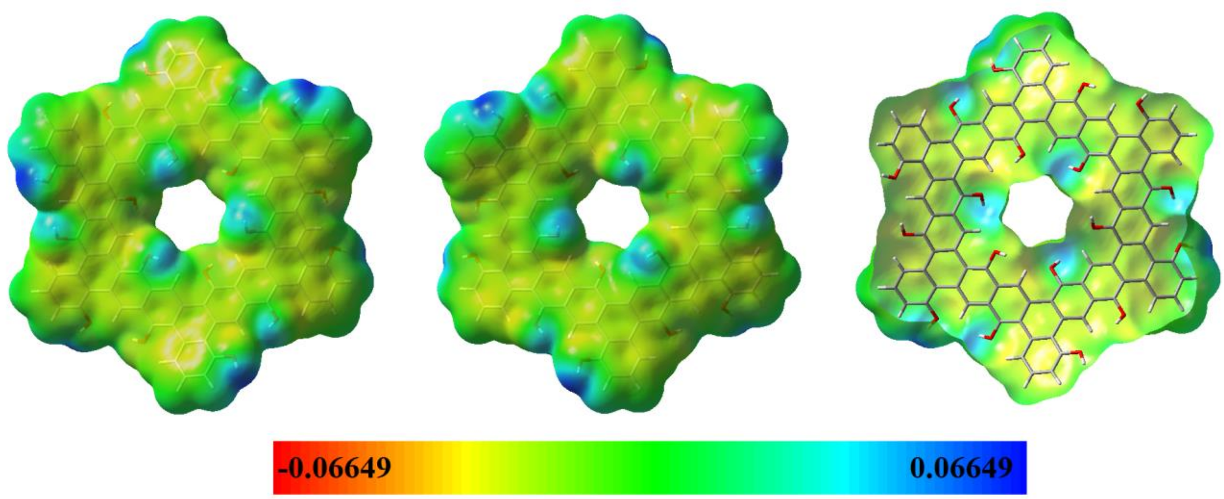

Figure S5. Electrostatic potential map (ESP) isosurfaces (isovalue of 0.0004 e/Å^3) of 6,6-H,OH nanosheet achieved at the B3LYP/6-31G(d,p) theoretical level, from three point of views.

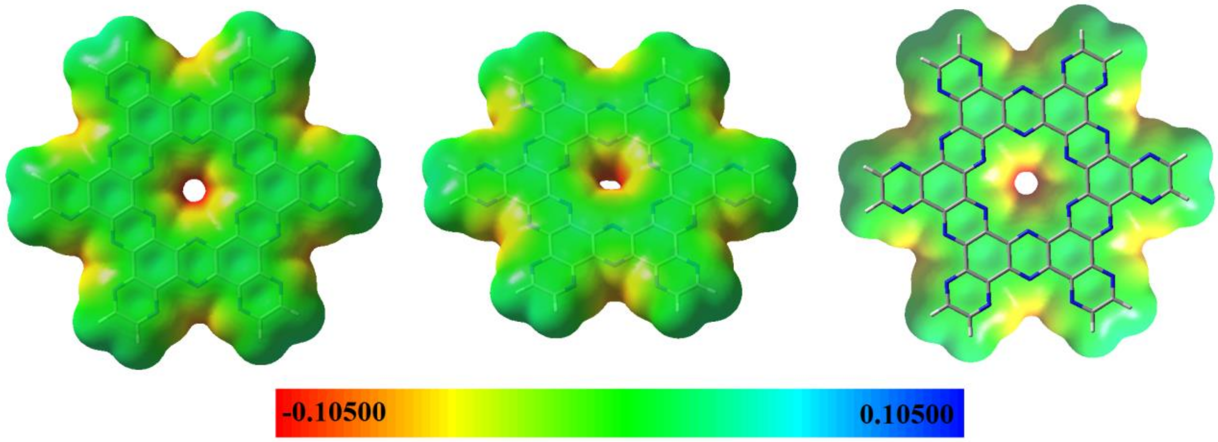

Figure S6. Electrostatic potential map (ESP) isosurfaces (isovalue of 0.0004 e/Å^3) of P-C_2N nanosheet achieved at the B3LYP/6-31G(d,p) theoretical level, from three point of views.

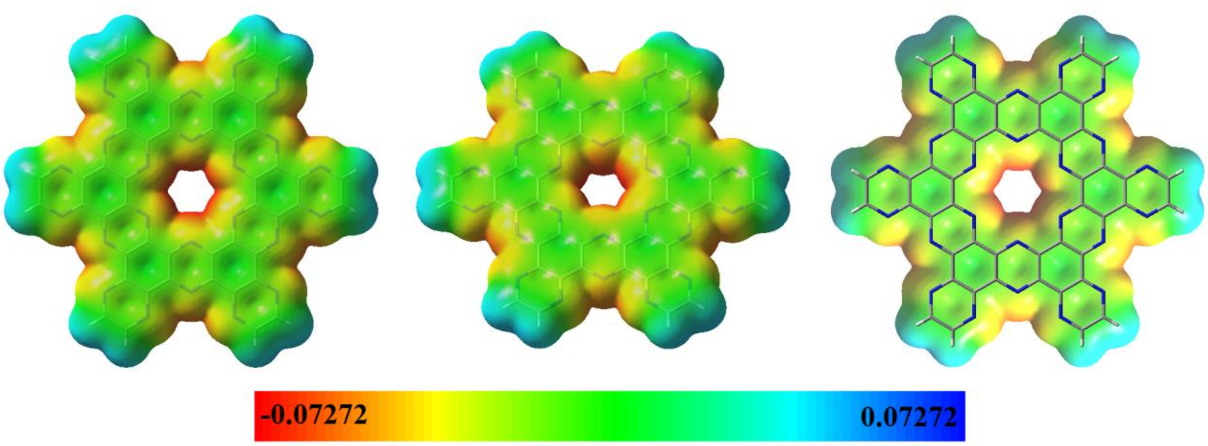

Figure S7. Electrostatic potential map (ESP) isosurfaces (isovalue of 0.0004 e/Å^3) of S-C_2N nanosheet achieved at the B3LYP/6-31G(d,p) theoretical level, from three point of views.

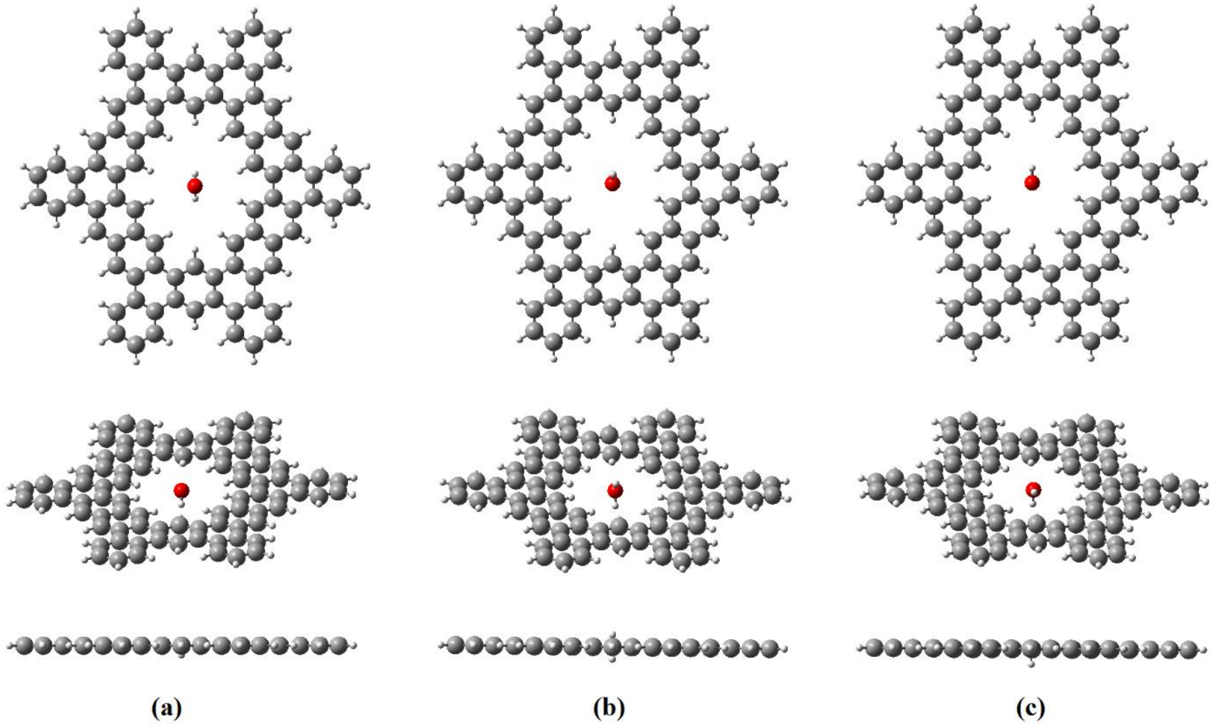

Figure S8. Top-, oblique- and side views of a water molecule passing through 10-H membrane via (a) mechanism I, (b) mechanism II, (c) mechanism III. The red, white, and gray spheres show O, H, and C atoms, respectively.

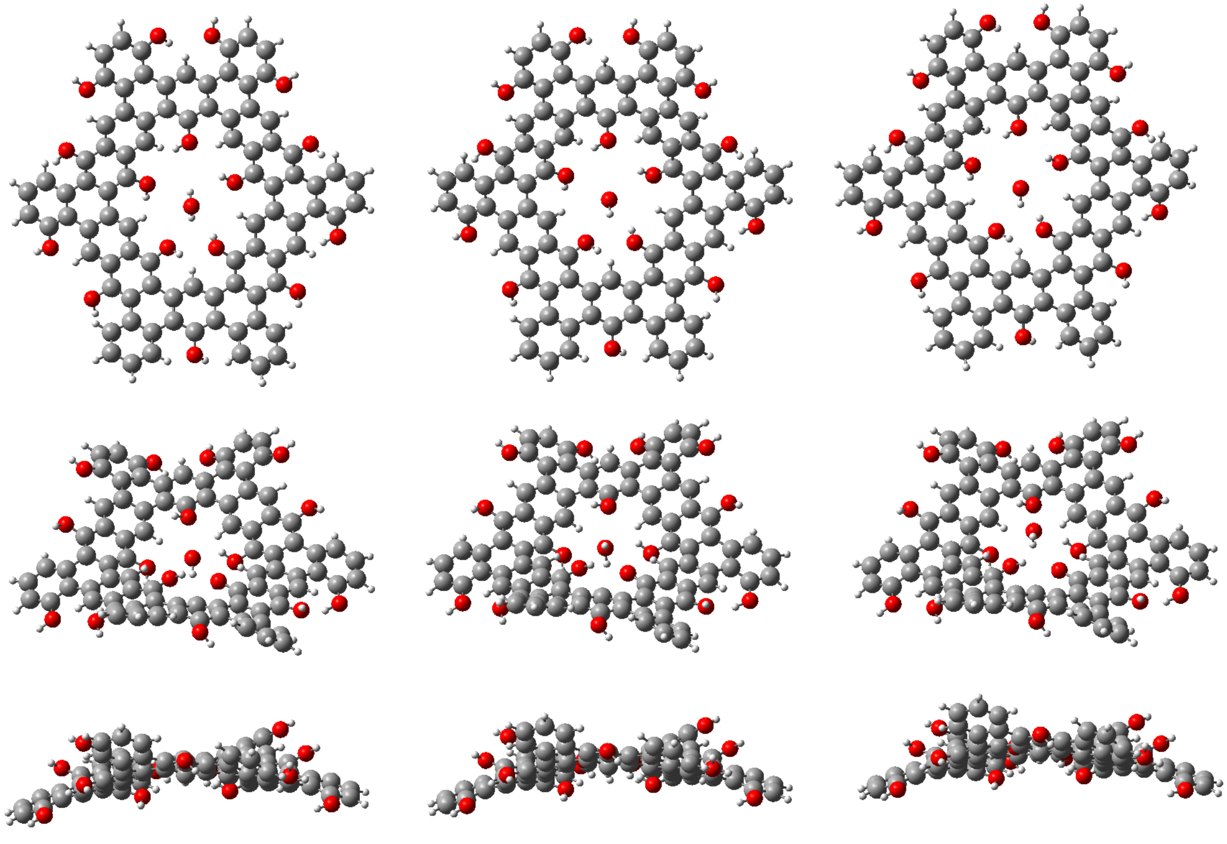

(a) (b) (c)

Figure S9. Top-, oblique- and side views of a water molecule passing through 5,5-H,OH membrane via (a) mechanism I, (b) mechanism II, (c) mechanism III. The red, white, and gray spheres show O, H, and C atoms, respectively.

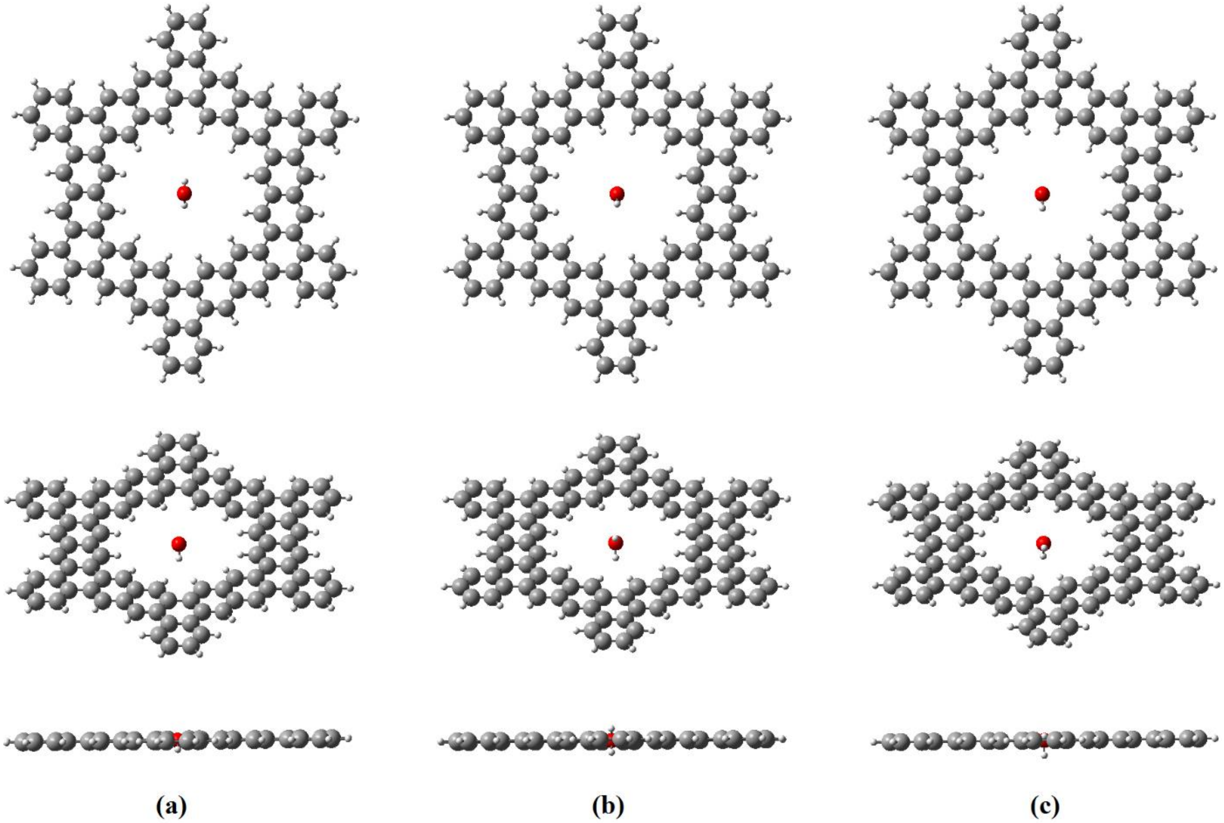

Figure S10. Top-, oblique- and side views of a water molecule passing through 12-H membrane via (a) mechanism I, (b) mechanism II, (c) mechanism III. The red, white, and gray spheres show O, H, and C atoms, respectively.

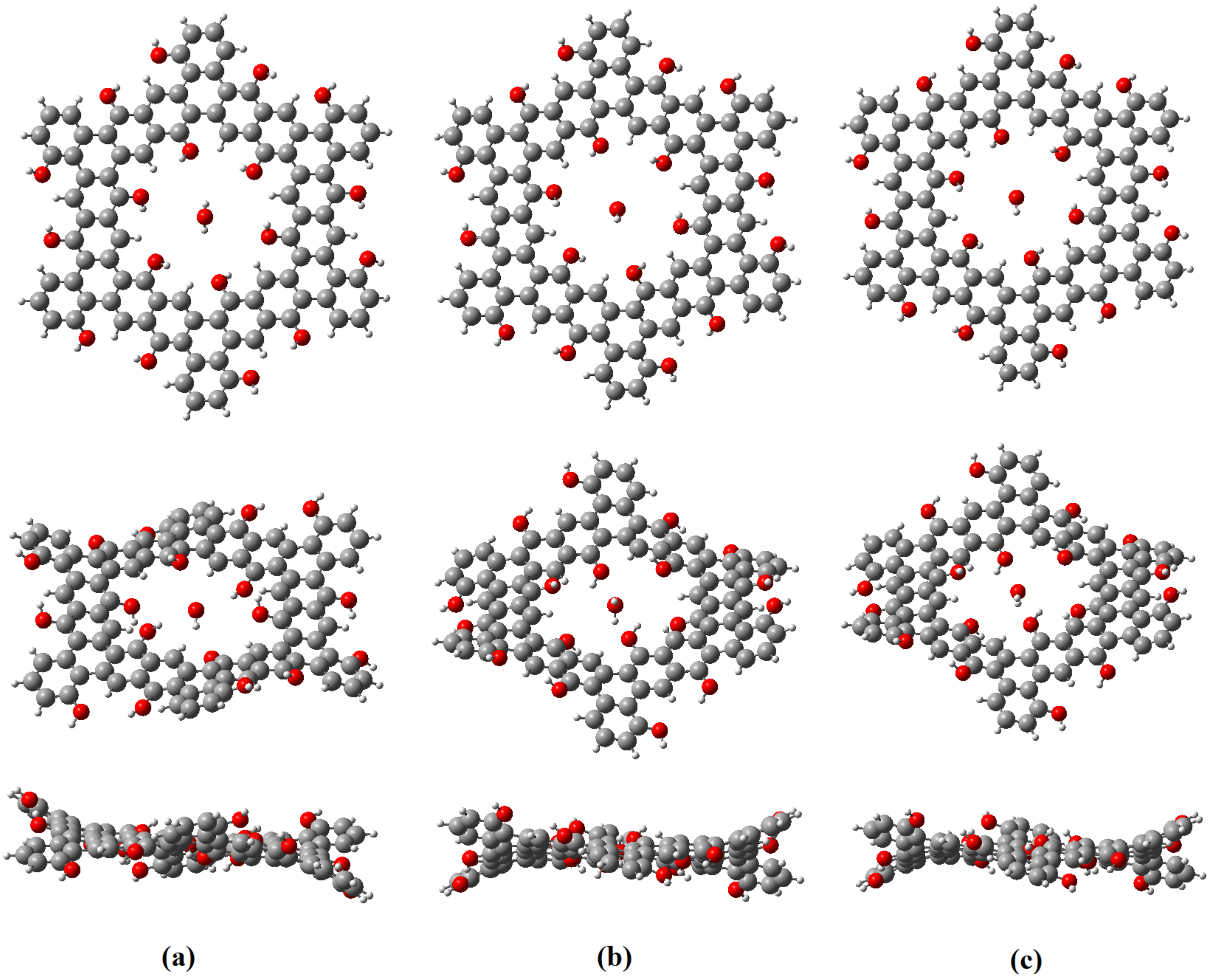

Figure S11. Top-, oblique- and side views of a water molecule passing through 6,6-H,OH membrane via (a) mechanism I, (b) mechanism II, (c) mechanism III. The red, white, and gray spheres show O, H, and C atoms, respectively.

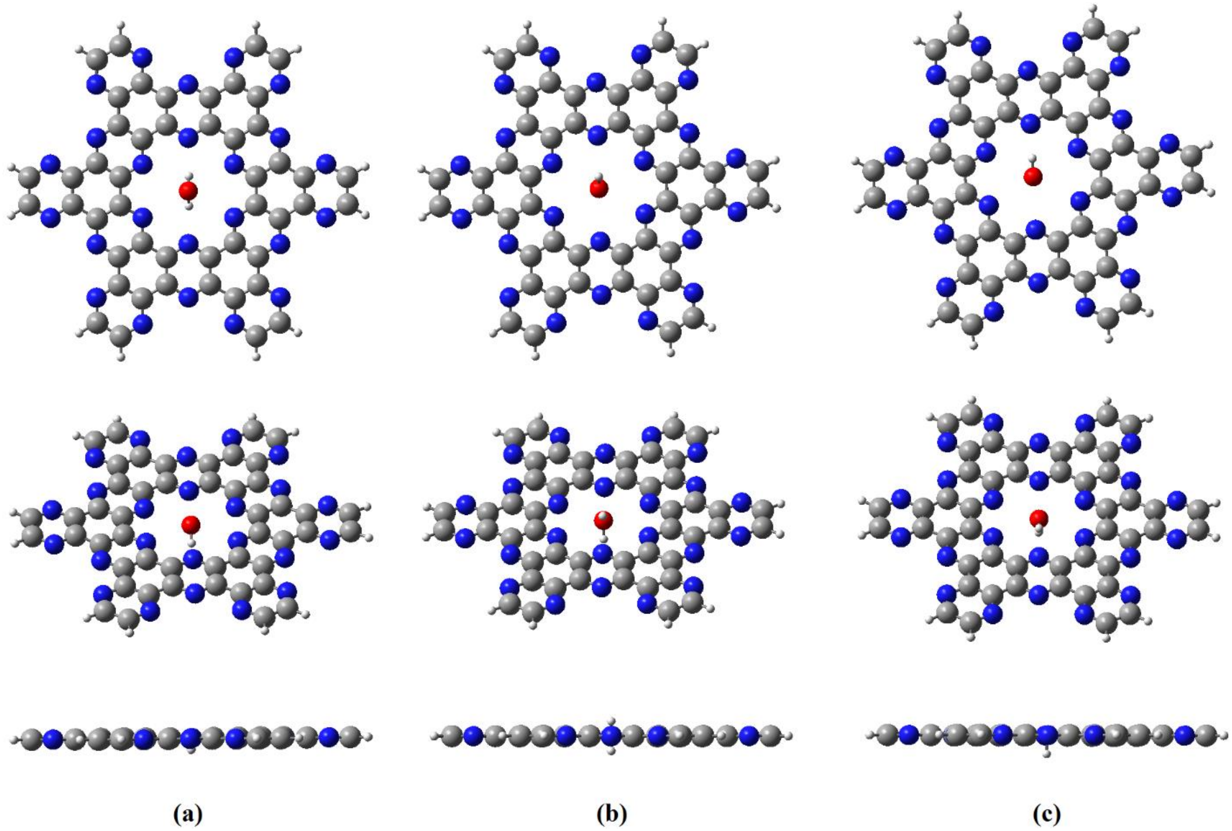

Figure S12. Top-, oblique- and side views of a water molecule passing through P-C_2N-I membrane via (a) mechanism I, (b) mechanism II, (c) mechanism III. The blue, red, white, and gray spheres show N, O, H, and C atoms, respectively.

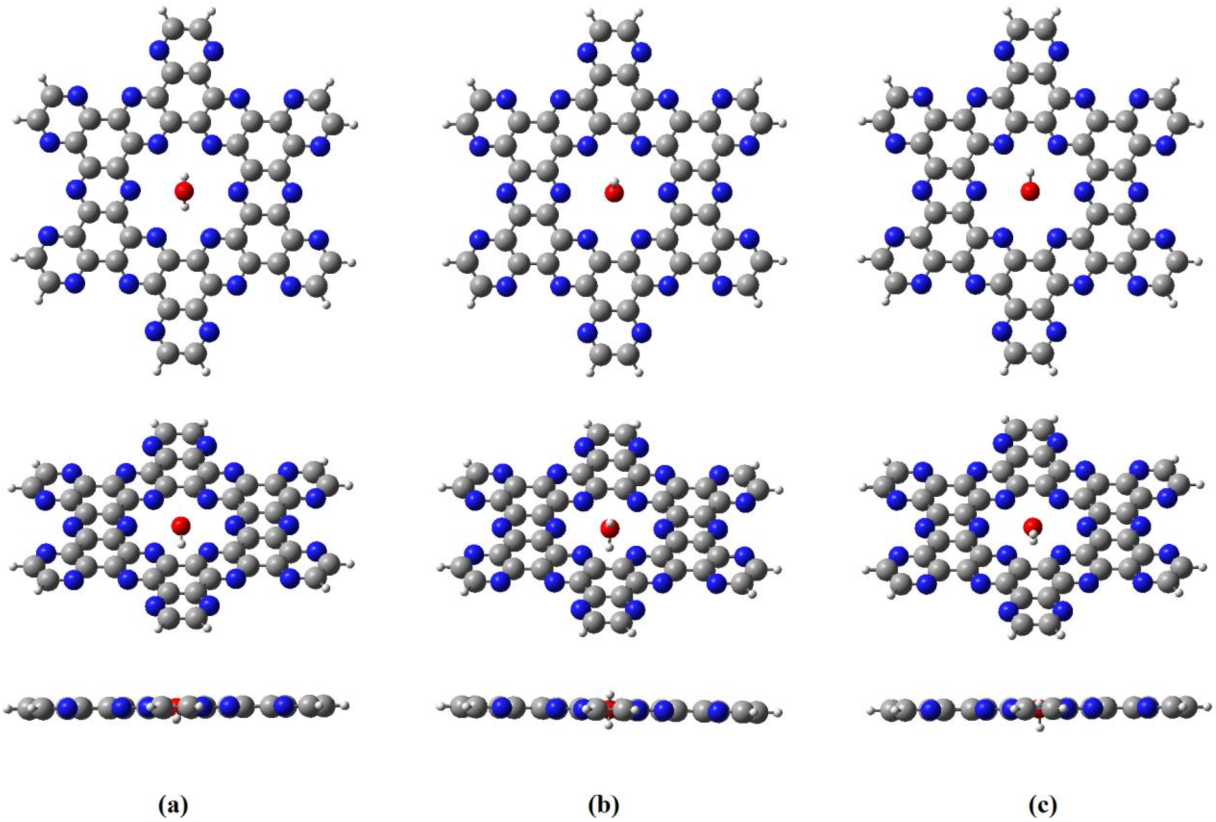

Figure S13. Top-, oblique- and side views of a water molecule passing through P-C_2N-II membrane via (a) mechanism I, (b) mechanism II, (c) mechanism III. The blue, red, white, and gray spheres show N, O, H, and C atoms, respectively.

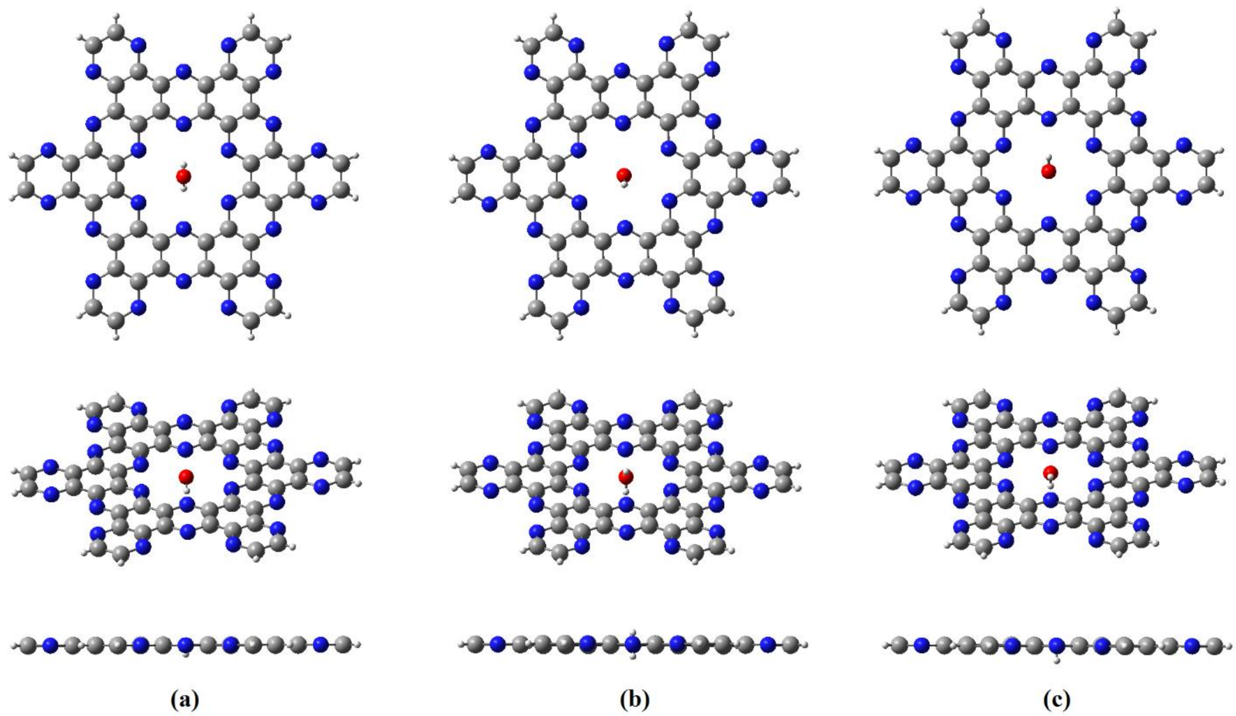

Figure S14. Top-, oblique- and side views of a water molecule passing through S-C_2N membrane via (a) mechanism I, (b) mechanism II, (c) mechanism III. The blue, red, white, and gray spheres show N, O, H, and C atoms, respectively.

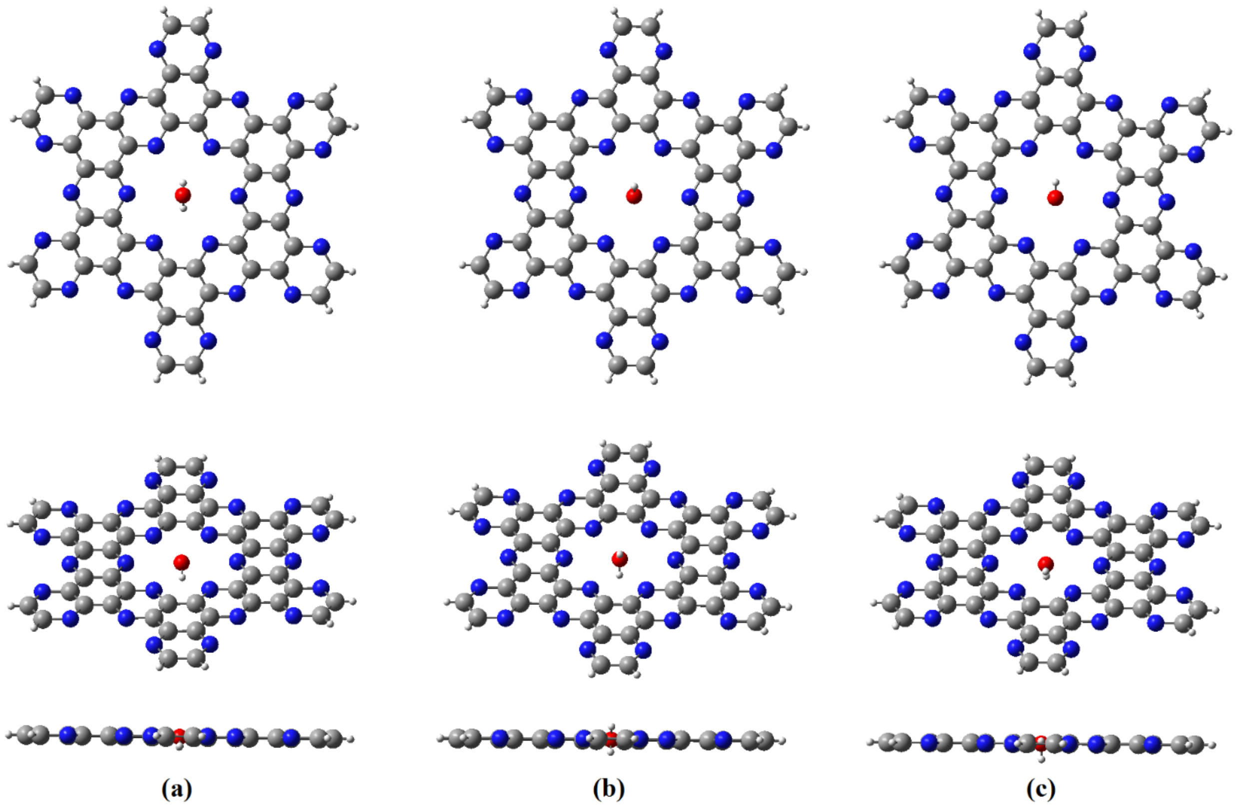

Figure S15. Top-, oblique- and side views of a water molecule passing through S-C_2N-II membrane via (a) mechanism I, (b) mechanism II, (c) mechanism III. The blue, red, white, and gray spheres show N, O, H, and C atoms, respectively.

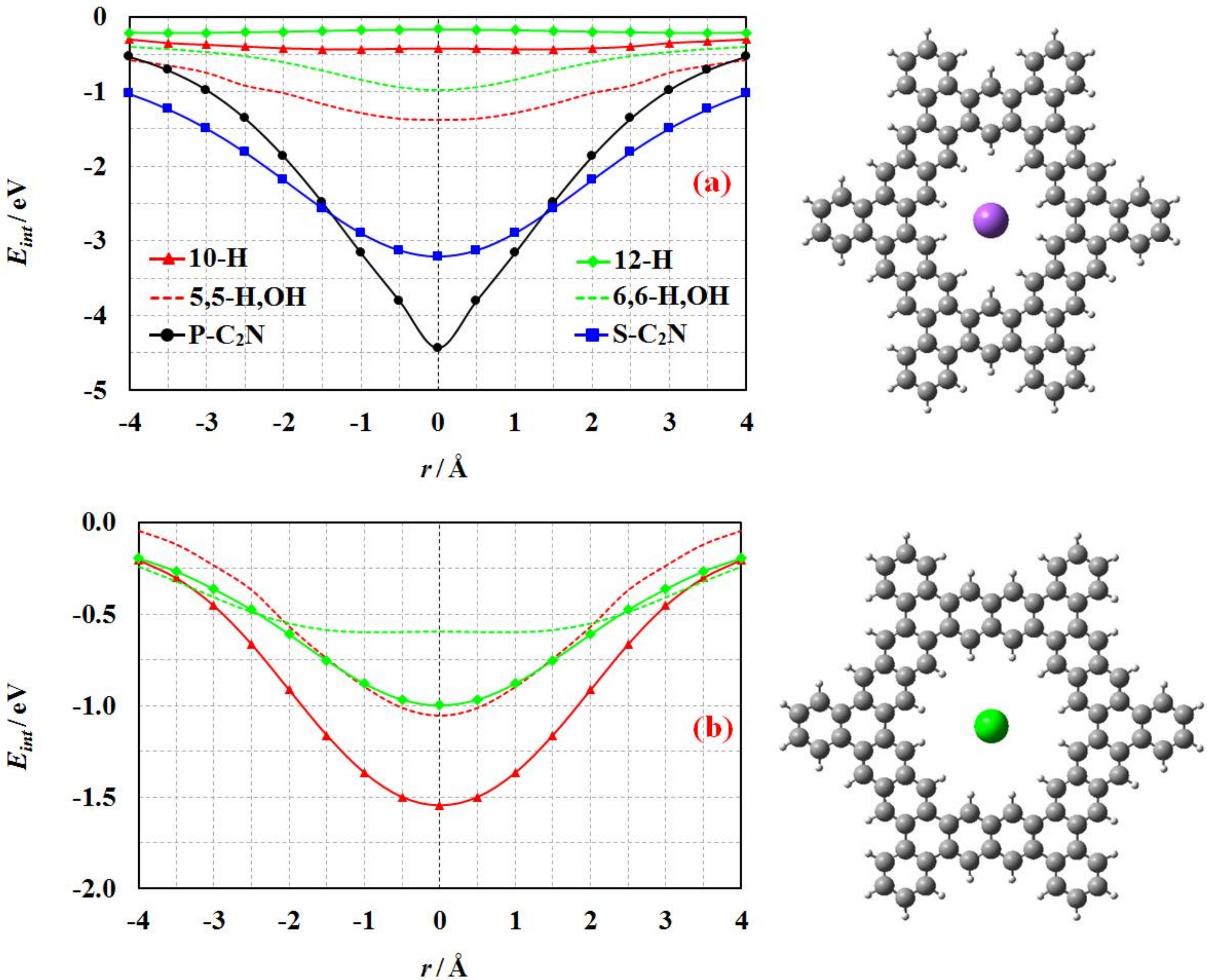

Figure S16. Interaction energies of Na^+ (a) and Cl^- ions (b) diffusing across target nanofilters obtained at the B3LYP/6-31G(d,p) level of theory.

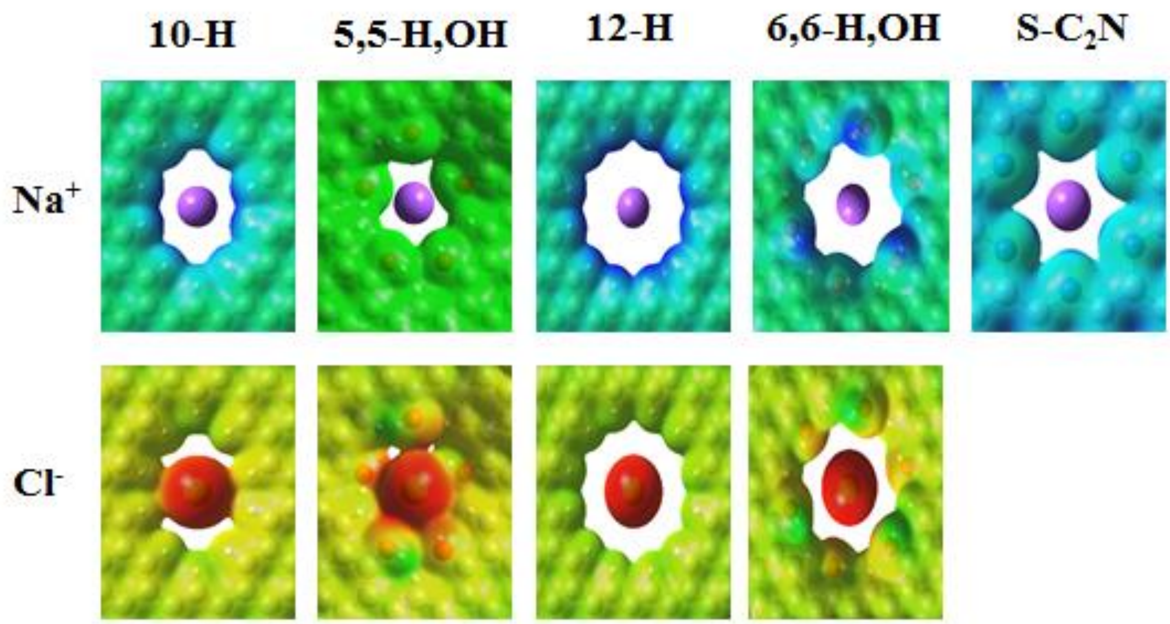

Figure S17. Electrostatic potential map (ESP) isosurfaces (isovalue of 0.004 e/Å^3) for Na^+ and Cl^- ions penetrating across chosen nanofilters obtained at the B3LYP/6-31G(d,p) level of theory.

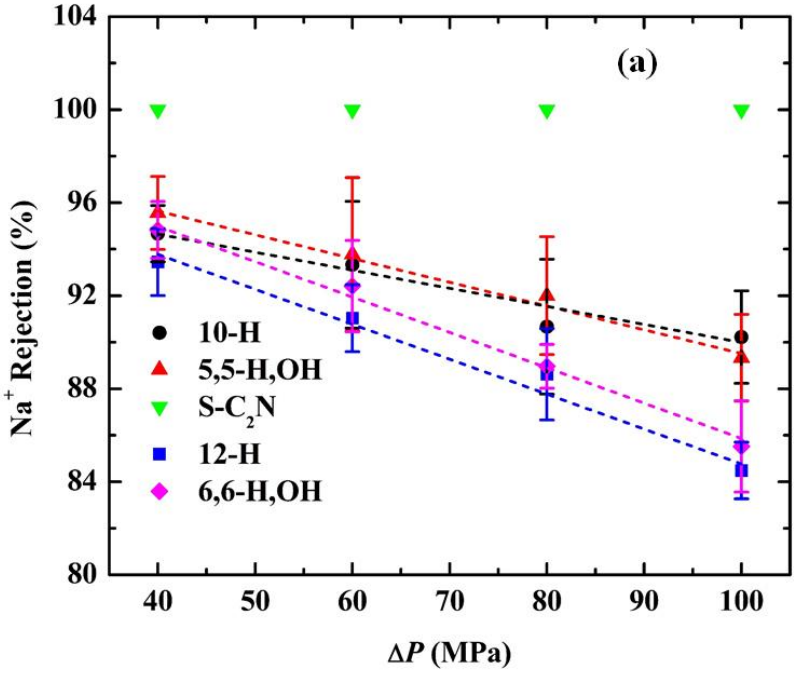

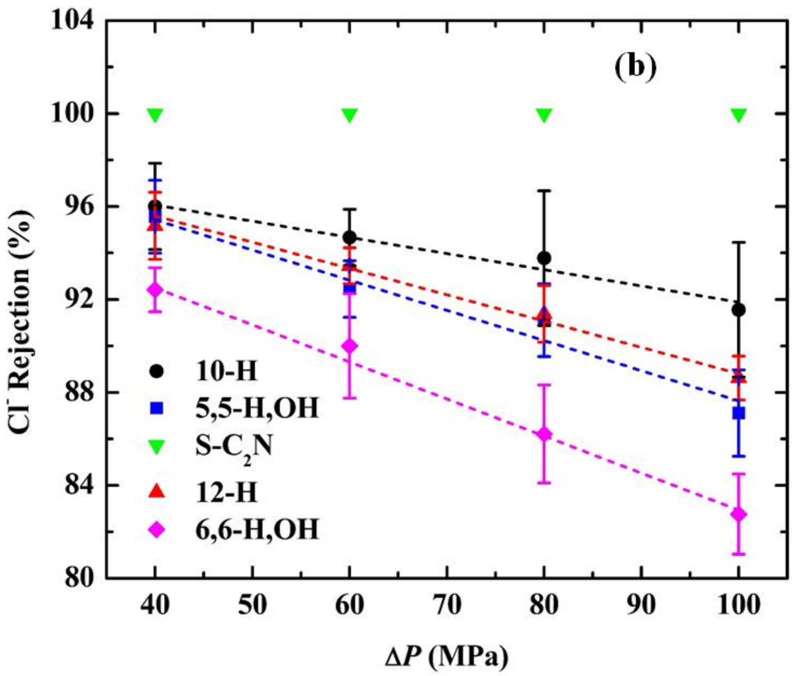

Figure S18. Ion rejection at pressures of 40, 60, 80 and 100 MPa for the selected nanosheets in the present work. Actually, $(1-N_p/N_f)\times100$ formula was used to calculate Na^+ and Cl^- rejection percentage, where N_p and N_f are the number of Na^+ or Cl^- in the permeate side at $t = 10$ ns and in the feed side at $t = 0$, respectively.

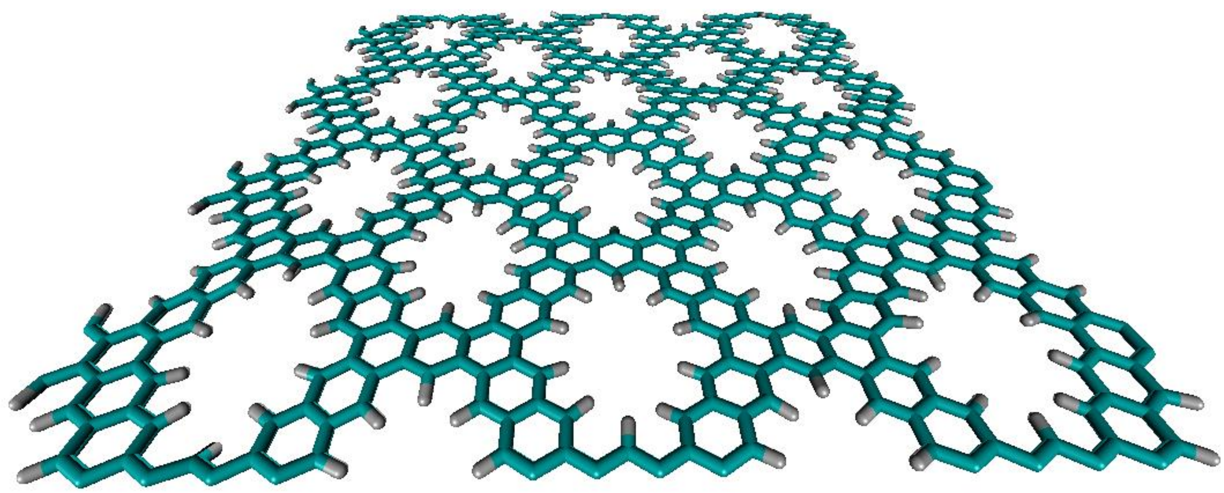

Figure S19. Side view of 10-H membrane at 100 MPa. The cyan and white spheres show C and H atoms, respectively.

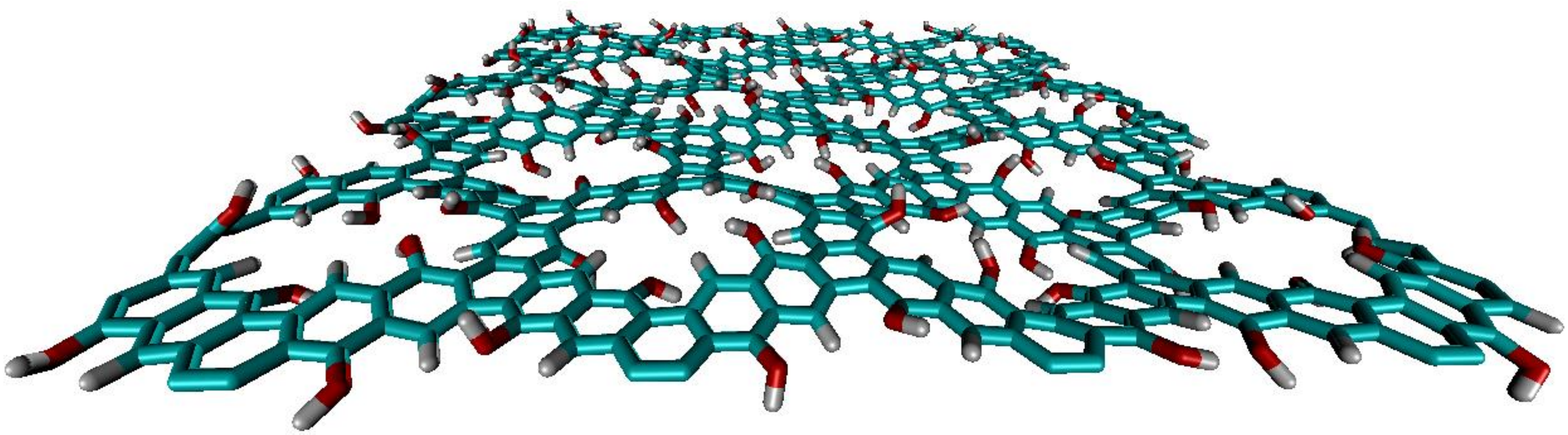

Figure S20. Side view of 5,5-H,OH membrane at 100 MPa. The cyan, red, and white spheres show C, O and H atoms, respectively.

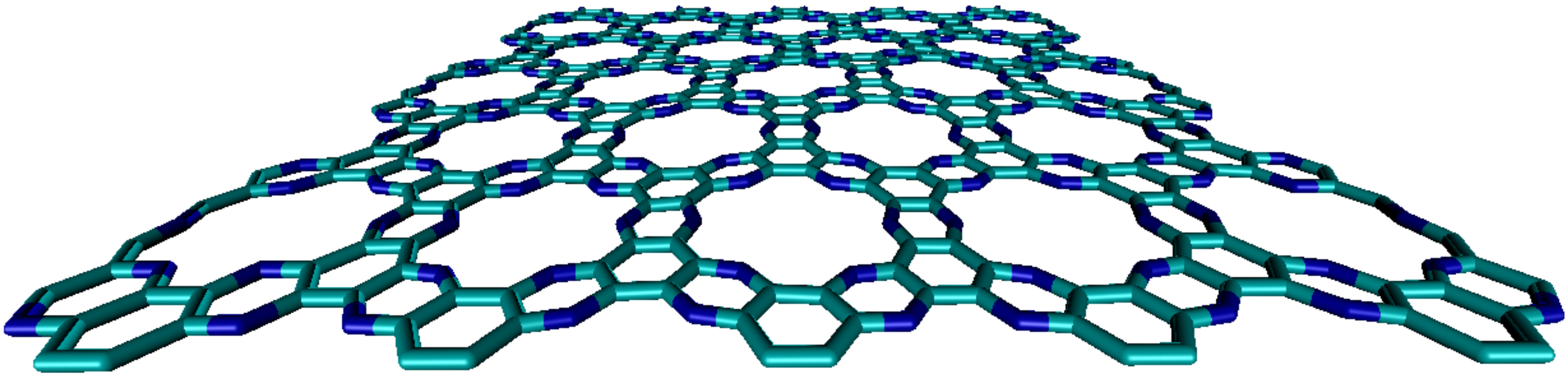

Figure S21. Side view of S-C_2N membrane at 100 MPa. The cyan and blue spheres show C and N atoms, respectively.

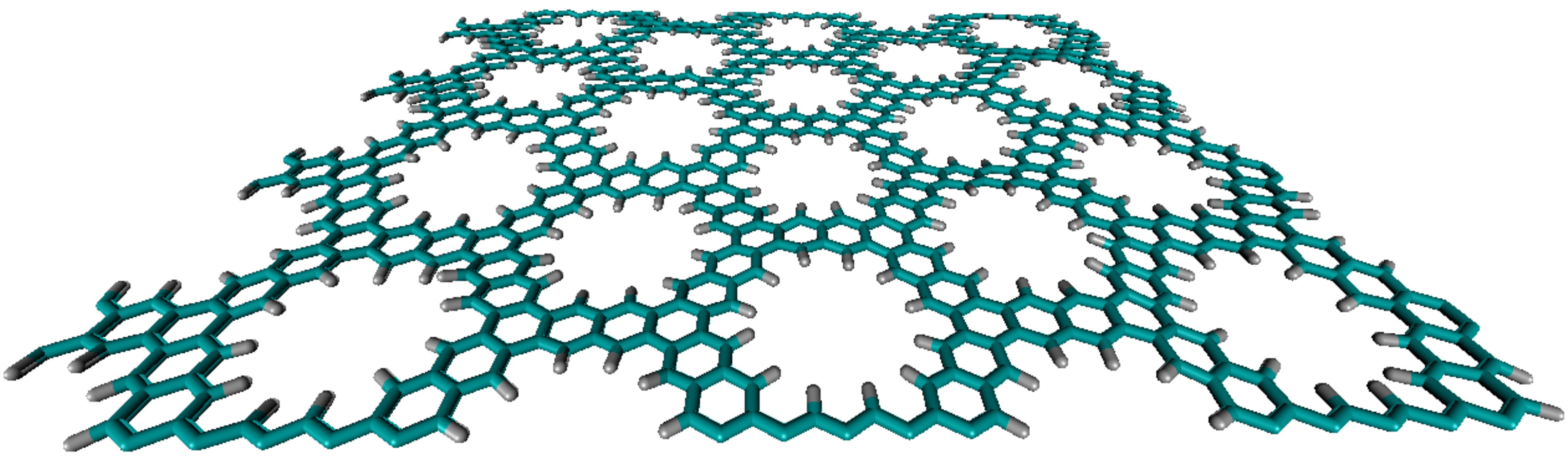

Figure S22. Side view of 12-H membrane at 100 MPa. The cyan and white spheres show C and H atoms, respectively.

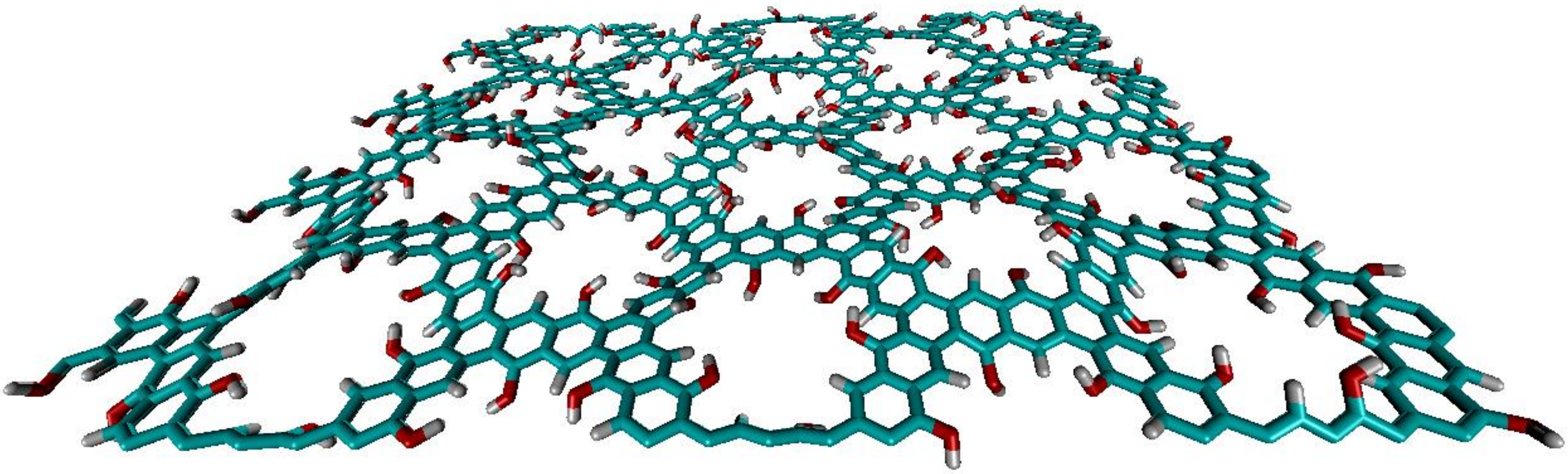

Figure S23. Side view of 6,6-H,OH membrane at 100 MPa. The cyan, red, and white spheres show C, O and H atoms, respectively.

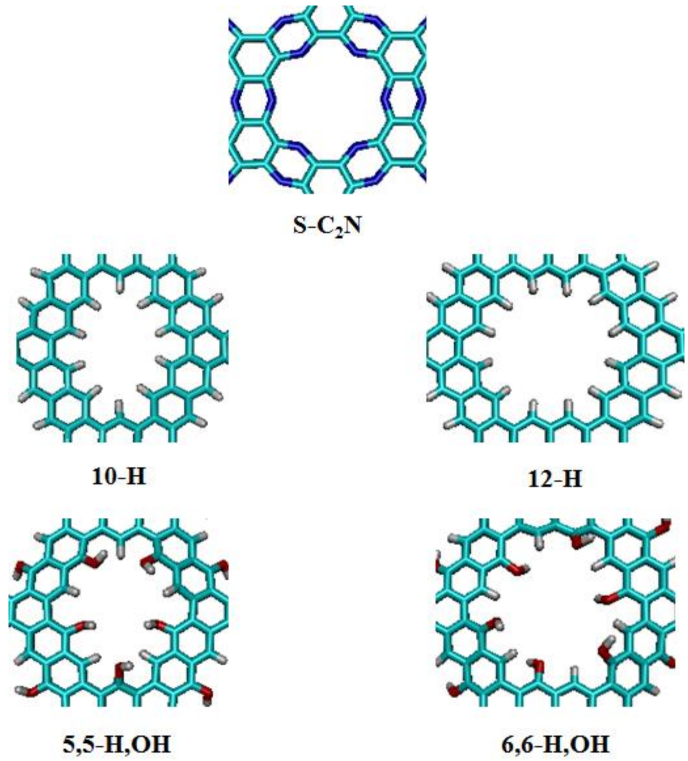

Figure S24. A snapshot of chosen nanopores at 100 MPa show the deformation at the their edge. The blue, cyan, red, and white spheres show N, C, O and H atoms, respectively.

References

(1) Joung, I. S.; Cheatham III; T. E. Determination of alkali and halide monovalent ion parameters for use in explicitly solvated biomolecular simulations. *J. Phys. Chem.* B **2008**, *112*, 9020-9041.

(2) Horn, H. W.; Swope, W. C.; Pitera, J. W.; Madura, J. D.; Dick, T. J.; Hura, G. L.; Head-Gordon, T. Development of an improved four-site water model for biomolecular simulations: TIP4P-Ew., *J. Chem. Phys.* **2004**, *120*, 9665.

(3) Beu, T. A. Molecular dynamics simulations of ion transport through carbon nanotubes. I. Influence of geometry, ion specificity, and many-body interactions. *J. Chem. Phys.* **2010**, *132*, 164513.

(4) Mooney, D. A.; Müller-Plathe, F.; Kremer, K. Simulation studies for liquid phenol: properties evaluated and tested over a range of temperatures. *Chem. Phys. Lett.* **1998**, *294*, 135-142.

(5) Müller-Plathe, F. Local structure and dynamics in solvent-swollen polymers. *Macromolecules* **1996**, *29*, 4782-4791.

(6) Lindorff-Larsen, K.; Piana, S.; Palmo, K.; Maragakis, P.; Klepeis, J. L.; Dror, R. O.; Shaw, D. E. Improved side-chain torsion potentials for the Amber ff99SB protein force field. *PROTEINS* **2010**, *78*, 1950-1958.